Journal of Molecular Cell Biology (2022), 14(1), mjac002
https://doi.org/10.1093/jmcb/mjac002
Published online January 11, 2022

Article

'C-type' closed state and gating mechanisms of K2P channels revealed by conformational changes of the TREK-1 channel

Qiansen Zhang[1,†], Jie Fu[1,†], Shaoying Zhang[1], Peipei Guo[1], Shijie Liu[1], Juwen Shen[1], Jiangtao Guo[2], and Huaiyu Yang[1,*]

[1] Shanghai Key Laboratory of Regulatory Biology, Institute of Biomedical Sciences, School of Life Sciences, East China Normal University, Shanghai 200241, China
[2] Department of Biophysics and Department of Pathology of Sir Run Run Shaw Hospital, Zhejiang University School of Medicine, Hangzhou 310058, China
[†] These authors contributed equally to this work.
* Correspondence to: Huaiyu Yang, E-mail: hyyang@bio.ecnu.edu.cn

Edited by Xuebiao Yao

Two-pore domain potassium (K2P) channels gate primarily within the selectivity filter, termed 'C-type' gating. Due to the lack of structural insights into the nonconductive (closed) state, 'C-type' gating mechanisms remain elusive. Here, molecular dynamics (MD) simulations on TREK-1, a K2P channel, revealed that M4 helix movements induce filter closing in a novel 'deeper-down' structure that represents a 'C-type' closed state. The 'down' structure does not represent the closed state as previously proposed and instead acts as an intermediate state in gating. The study identified the allosteric 'seesaw' mechanism of M4 helix movements in modulating filter closing. Finally, guided by this recognition of K2P gating mechanisms, MD simulations revealed that gain-of-function mutations and small-molecule activators activate TREK-1 by perturbing state transitions from open to closed states. Together, we reveal a 'C-type' closed state and provide mechanical insights into gating procedures and allosteric regulations for K2P channels.

Keywords: K2P, state, selectivity filter, C-type, gating

Introduction

Potassium channels play a fundamental role in controlling K^+ ion permeation across the cell membrane and have been implicated in numerous biological functions, including electric signaling in the nervous system and the regulation of neuronal firing, muscle contraction, hormones, neurotransmitters, and enzyme secretion (Gonzalez et al., 2012; Tian et al., 2014). Despite their structural diversity, all these ion channels share the structural property of having a selectivity filter (SF) near the extracellular side and a helix-bundle crossing near the intracellular side. In general, most potassium channels use the conventional gating mechanism in which the helix-bundle crossing controls channels to open or close in response to a variety of stimuli (Cordero-Morales et al., 2006; Cuello et al., 2010a, b).

Potassium channels are classified into four main types: voltage-gated K^+ (Kv) channels, Ca^{2+}-dependent K^+ (K_{Ca}) channels, inwardly rectifying K^+ (Kir) channels, and two-pore domain K^+ (K2P) channels (Wulff et al., 2009; Tian et al., 2014). K2P channels assemble as dimers, differently from other K^+ channels, which are tetramers. Each subunit of a K2P channel contains four transmembrane helices (M1–M4), two pore-forming loops (P1 and P2), two selectivity filter strands (SF1 and SF2), and a large intracellular region (Brohawn et al., 2012; Dong et al., 2015; Lolicato et al., 2017, 2020; Pope et al., 2020). The 15 members of the K2P family are divided into 6 subfamilies: TWIK (tandem of pore domains in a weak inwardly rectifying K^+ channel), TREK (TWIK-related K^+ channel), TASK (TWIK-related acid-sensitive K^+ channel), TALK (TWIK-related alkaline-pH-activated K^+ channel), TRESK (TWIK-related spinal-cord K^+ channel), and THIK (tandem-pore-domain halothane-inhibited

Received November 22, 2021. Revised January 4, 2022. Accepted January 7, 2022.
© The Author(s) (2022). Published by Oxford University Press on behalf of *Journal of Molecular Cell Biology*, CEMCS, CAS.
This is an Open Access article distributed under the terms of the Creative Commons Attribution-NonCommercial License (https://creativecommons.org/licenses/by-nc/4.0/), which permits non-commercial re-use, distribution, and reproduction in any medium, provided the original work is properly cited. For commercial re-use, please contact journals.permissions@oup.com

K^+ channel) (Goldstein et al., 2001, 2005). Few K2P channels, such as TASK-1 and TASK-2, show gating at the helix-bundle crossing (Li et al., 2020; Rodstrom et al., 2020). The conformations of the open and closed gates of these K2P channels at the helix-bundle crossing have been well characterized (Li et al., 2020; Rodstrom et al., 2020). However, most K2P members, such as the TREK subfamily, adopt a 'C-type' gating mechanism where the channels gate primarily within the filter (Bagriantsev et al., 2011, 2012; Piechotta et al., 2011; Schewe et al., 2016; Lolicato et al., 2017). For these 'C-type' gating K2P channels, the structure with the open filter has been reported, whereas the 'C-type' closed state with the closed filter remains to be elucidated.

The TREK subfamily, a model system for the structure and function study of K2P channels, generates 'leak' currents that regulate neuronal excitability and influence pain, depression, temperature perception, and anesthetic responses (Mathie et al., 2010, 2021; Feliciangeli et al., 2015; Douguet and Honore, 2019). The M4 helix plays critical roles in connecting stimuli and filter conformation changes, since its C-terminus forms a continuous helix with the C-tail that senses stimuli, including phospholipids, phosphorylation, temperature, and pressure, and its N-terminus couples P1 of the filter region (Bagriantsev et al., 2011; Piechotta et al., 2011; Lolicato et al., 2014; Schewe et al., 2016). Prior structural studies have revealed that M4 movements cause two different structures of K2P channels, the so-called 'up' and 'down' structures (Brohawn et al., 2012, 2013; Lolicato et al., 2014; Dong et al., 2015). The 'up' structure is achieved primarily by the upward movement and rotation of M4, resulting in the C-terminal part of M4 packing against M2 and the closure of the side fenestrations. In the 'down' structure, M4 is approximately straight, crosses the membrane at an ∼45° angle and does not interact with M2 (Brohawn et al., 2012, 2013; Lolicato et al., 2014; Dong et al., 2015). MD simulations showed that the TREK-2 channel moves from the 'down' to the 'up' structure in response to membrane stretching (Aryal et al., 2017; Brennecke and de Groot, 2018).

Conductive filter conformation and disulfide crosslinking studies have indicated that the 'up' structure represents the open state of K2P channels (Brohawn et al., 2014; Dong et al., 2015). The 'down' structure is thought to represent the closed state (Brohawn et al., 2014; Dong et al., 2015). However, crystallography studies have not supported this view, as the 'down' structure shows a conductive filter identical to the 'up' structure (Brohawn et al., 2014; Dong et al., 2015). Consequently, due to the lack of structural information on the nonconductive (closed) state, K2P 'C-type' gating has not been characterized, and much remains to be learned about how ligands or mutations influence K2P channel activities.

Combining steered and conventional MD simulations on TREK-1, in this study, we investigated whether and how M4 helix movements can allosterically modulate filter gating. We identified a novel TREK-1 closed structure that has a nonconductive filter. We revealed the gating mechanisms of the transition from open to closed TREK-1. Finally, based on the gating mechanisms, we elucidated the mechanisms of ligand activation and gain-of-function mutations.

Results

The transition of the TREK-1 channel to a novel 'C-type' closed conformation

First, we placed the TREK-1 'up' state structure (PDB code: 6CQ8) (Lolicato et al., 2017) in a palmitoyl-oleoyl-phosphatidylcholine (POPC) phospholipid bilayer and performed three independent 500-ns conventional MD simulations. Referring to a previous study (Aryal et al., 2017), the motions of the M4 helix could be defined by three distances among helices M2, M3, and M4: (i) the 'fenestration' distance between Gly293 on M4 and Pro168 on M2 of the adjacent subunit; (ii) the 'zipper' distance between Trp295 on M4 and Arg207 on M3 of the same subunit; and (iii) the 'expansion' distance between Met291 on M4 and Gly182 on M2 of the same subunit (Supplementary Figure S1A). In the MD simulations, the channel was kept in a stable 'up' conformation with a 'fenestration' distance of 5.6 Å, 'zipper' distance of 14.8 Å, and 'expansion' distance of 13.1 Å (Supplementary Figure S1A–D). In the simulations, the filter maintained in a conductive conformation similar to the crystal structure (Lolicato et al., 2017; Supplementary Figure S1E and F).

Next, a steered MD (SMD) simulation was performed in uniaxial tension with an external force applied to the N-terminal part of the M4 helix along the direction parallel to the POPC bilayer to enable a transition of the TREK-1 channel from the 'up' conformation to other conformations (Figure 1A). The 'fenestration', 'zipper', and 'expansion' distances of the channel exhibited pronounced fluctuations and dramatic variations in the SMD simulation (Figure 1B). According to the three distances, the conformations of TREK-1 could be divided into three states (Figure 1B). During the initial 100 ns, the channel was in the 'up' state with the 'fenestration' distance stabilized at ∼5.0 Å. During the simulation of 100–290 ns, as the C-terminus of M4 moved downward, the 'fenestration' distance gradually increased to ∼9.0 Å and stabilized for a period, and the 'zipper' and 'expansion' distances were stabilized at ∼9.0 or 8.0 Å. Such distances of TREK-1 became similar to the distances in the crystal 'down' structure (Dong et al., 2015) and different from the crystal 'up' structure (Dong et al., 2015; Lolicato et al., 2017; Figure 1C). During the last 200 ns of the simulation, the M4 helix further moved downward and was transformed to a 'deeper-down' conformation whose distance was distinct from those of the 'up' and 'down' structures. The 'fenestration' distance further increased to ∼12 Å and the 'expansion' distance further decreased to ∼6 Å (Figure 1B). Furthermore, we found that the filter changed from a conductive conformation to a nonconductive conformation (Figure 1D). This phenomenon indicated that M4 helix movements may affect the switching of the filter conformation. We then analyzed potential relationships between their dynamics. A cluster analysis of the SMD trajectory was performed with two variables (Figure 1E): (i) the distant SF diameter defined by the greatest distance of the four Oγ–Oγ pairs forming the

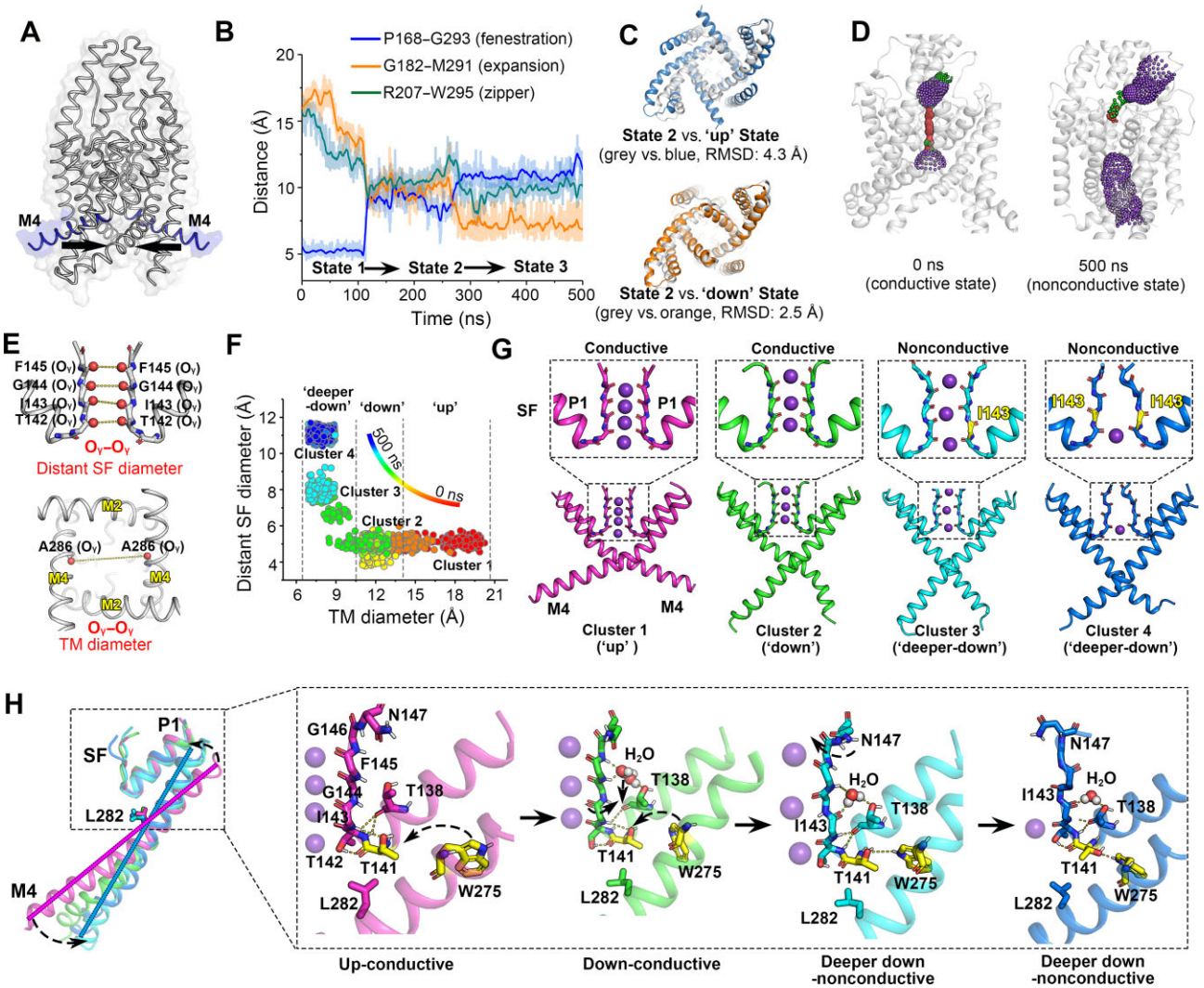

Figure 1 Conformation transitions of the TREK-1 channel from the 'up' to 'deeper-down' structure in the SMD simulation. (**A**) Schematic diagram of stretching M4 helix in the simulation. (**B**) Changes in 'fenestration' (blue), 'zipper' (green), and 'expansion' (yellow) distances in the simulation. (**C**) Superimposition of the state 2 conformation (gray) and the 'up' (blue) or 'down' (orange) structures. (**D**) Pore radius of the initial and final snapshots of the simulation. (**E**) Definitions of the distant SF diameter and TM diameter. (**F**) Cluster analysis of the SMD trajectories with the distant SF diameter and TM diameter as two variables. (**G**) Typical conformations. (**H**) The 'seesaw' movements of M4 and the influences of the movements on the networks within the filter region. Potassium ions and water molecules in the SF region are shown as purple or red spheres. Key residues are highlighted by colored sticks. Potential hydrogen bonds are indicated by dotted lines. Directions of conformational changes are indicated by dashed arrows.

central filter pore; and (ii) the TM diameter defined by the distance between the Oγ atoms of A286 from two subunits. These two variables represent filter and M4 dynamics, respectively. According to the TM diameter, the SMD conformations could be clustered into three groups: 'up', 'down', and 'deeper-down' (Figure 1F). This result is similar to the clustering using the three distances (Figure 1B). The filter in the 'up' and 'down' groups was in the conductive state with a distant SF diameter of 5 Å (Figure 1F and G; Supplementary Figure S2A and B). The distant SF diameter of the 'deeper-down' groups was much greater than 5 Å, suggesting that the Oγ atoms forming the central filter pore fluctuated in the simulations (Figure 1F and G; Supplementary Figure S2A and B). In particular, the backbone carbonyl group of I143 from the filter frequently underwent dynamic reorientations by 180° and then caused a nonconductive filter conformation (Figure 1G).

When the channel transformed from the 'up' to 'deeper-down' structure in the SMD simulation, the M4 helix appeared like a seesaw. Taking L282 as the fulcrum, the C-terminus of the M4 segment of the channel swung downward in the simulation, whereas the N-terminus swung in the opposite direction (Figure 1H). In the 'up' and 'down' structures, the OH group of T141 forms a hydrogen bond with the NH group of I143. When the M4 N-terminus squeezed to the P1 region in the

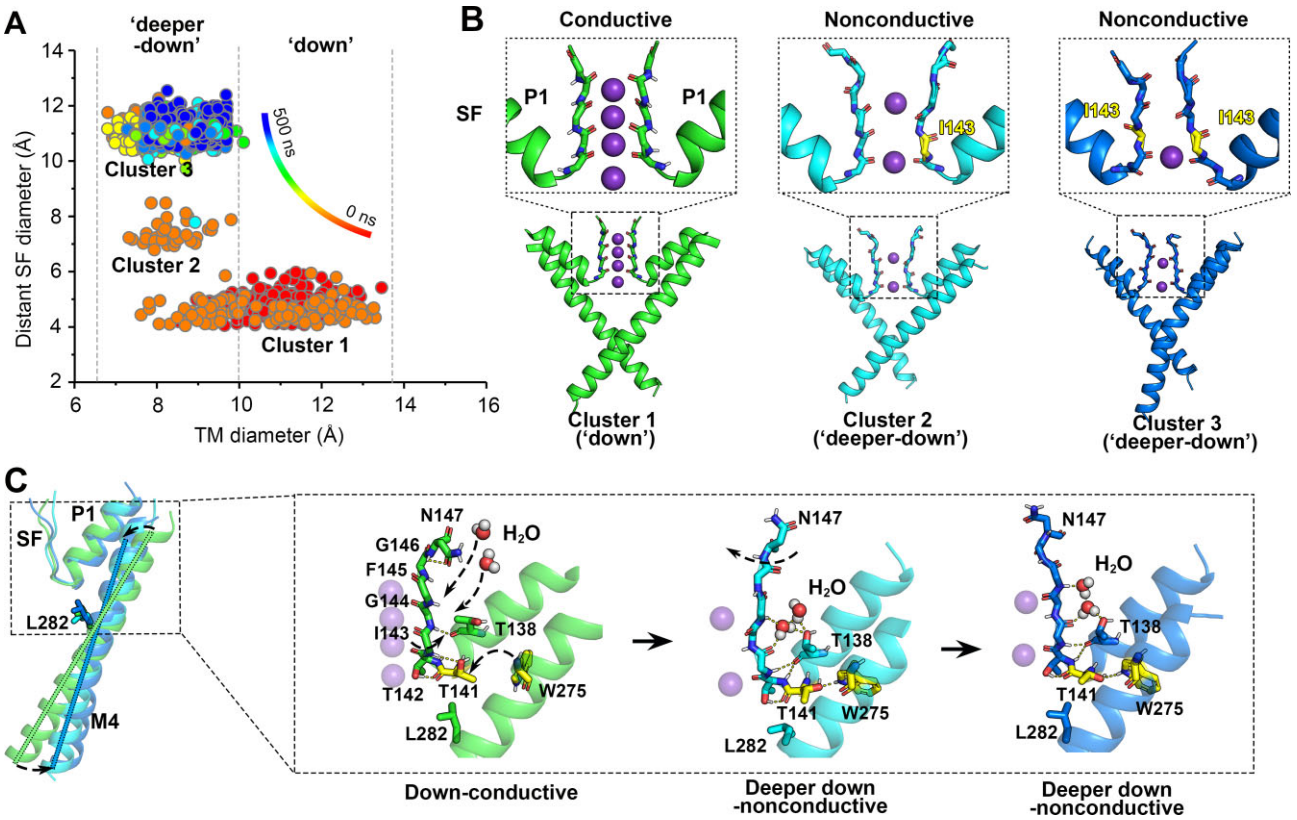

Figure 2 Conformation transitions of the TREK-1 channel from the 'down' to 'deeper-down' structure in the MD simulation. (**A**) Cluster analysis of the MD simulation trajectory with the distant SF diameter and TM diameter as two variables. (**B**) Typical conformations. (**C**) The 'seesaw' movements of M4 and the influences of the movements on the networks within the filter region.

'deeper-down' structure, the fluctuating side chain of W275 competed with I143 to interact with T141. Finally, the W275–T141 hydrogen bond was formed, whereas the I143–T141 hydrogen bond disappeared (Figure 1H). Consequently, the networks stabilizing the conductive filter were disturbed and the filter changed into nonconductive conformations (Figure 1H).

Validation in the transition from 'down' to 'deeper-down' by a conventional MD simulation

The SMD simulation suggested that the 'down' structure could change to a 'deeper-down' structure. Next, we are interested in whether this transition could be captured by conventional MD simulation. We then performed three independent 500-ns MD simulations by placing the 'down' structural model of the TREK-1 channel (Supplementary Figure S3) in a POPC phospholipid bilayer. During the initial stages, the channel was kept in the 'down' conformation with a 'fenestration' distance of ~10 Å, 'zipper' distance of ~9 Å, and 'expansion' distance of ~8 Å (Supplementary Figure S4A–D). In the remaining simulation trajectories, the 'fenestration', 'zipper', and 'expansion' distances are approximately 12, 9, and 5 Å, respectively (Supplementary Figure S4A–D). This distance profile of MD conformations is similar to that of the 'deeper-down' structure (Figure 1B), suggesting that the M4 helix moved to the 'deeper-down' conformation in the simulations. The clustering using the TM diameter and the distant SF diameter as variables also supports this (Figure 2A). In the MD simulations, the K2P structures with the 'down' M4 showed the conductive filter conformation. When TREK-1 transited to the 'deeper-down' structure in the simulations, the filter became nonconductive (Figure 2B; Supplementary Figure S4E and F). The conventional MD simulations also corroborate the M4 helix acting as a seesaw. In the transition of the 'down' to 'deeper-down' structures, W275 formed an interaction with T141 and disrupted the contact between T141 and I143 (Figure 2C). Therefore, the action mechanisms for the allosteric modulation of M4 on the filter in the conventional MD simulation are identical to those driven from the above SMD simulation.

Action mechanisms of gain-of-function mutations on channel gating

W275S is a gain-of-function mutation of TREK-1 that recovers current by increasing the single channel open probability (Bagriantsev et al., 2011). The above simulations suggested critical roles of W275 in 'C-type' gating. We next performed an SMD simulation on W275S to explore the precise impact of gain of function on TREK-1 channel activity. The movements of the M4 helix and the filter were analyzed (Figure 3A–E;

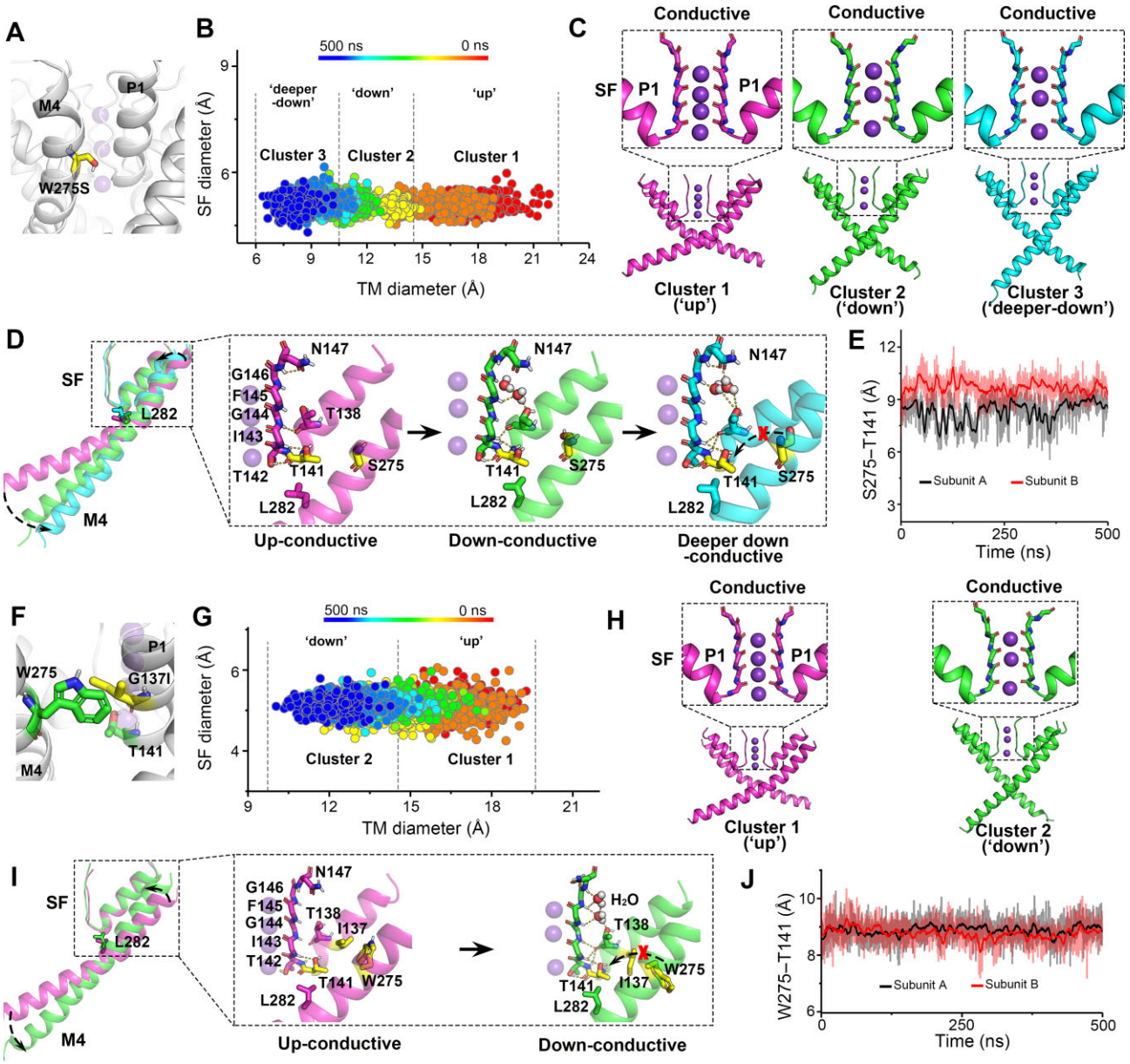

Figure 3 Conformation transitions of the channel in the SMD simulations of the gain-of-function mutants W275S and G137I. (**A**) Mapping of the mutant W275S in the 'up' state of the TREK-1 channel. The Ser residue is shown. (**B**) Cluster analysis of the W275S SMD trajectory with the distant SF diameter and TM diameter as two variables. (**C**) Typical conformations of the W275S SMD trajectory. (**D**) The 'seesaw' movements of M4 and the influences of the movements on the networks within the filter region. (**E**) Time traces of distances between the hydroxyl group of S275 and the hydroxyl group of T141 during the W275S SMD simulation. (**F**) Mapping of the mutant G137I in the 'up' state of the TREK-1 channel. A few of the residues are highlighted by the green sticks. (**G**) Cluster analysis of the G137I SMD trajectory with the distant SF diameter and TM diameter as two variables. (**H**) Typical conformations of the G137I SMD trajectory. (**I**) The 'seesaw' movements of M4 and the influences of the movements on the networks within the filter region. The display form is shown as in **D**. (**J**) Time traces of distances between the indole NH group of W275 and the hydroxyl group of T141 during the G137I SMD simulation.

Supplementary Figure S5). Regarding M4 helix movements, the W275S mutant showed the transition from the 'up' to 'deeper-down' structure with the 'down' structure as an intermediate state (Figure 3B and C). The 'up' and 'down' structures of the W275S mutant are similar to those of wild-type (WT) TREK-1. However, unlike WT TREK-1, the 'deeper-down' structure of W275S contained a conductive filter (Figure 3C and D; Supplementary Figure S5C and D). The mechanisms underlying these phenomena are that S275 could not interact with T141 as W275 did in the WT (Figure 3D and E). Therefore, T141 still interacted with I143, and the networks stabilizing the conductive filter were retained.

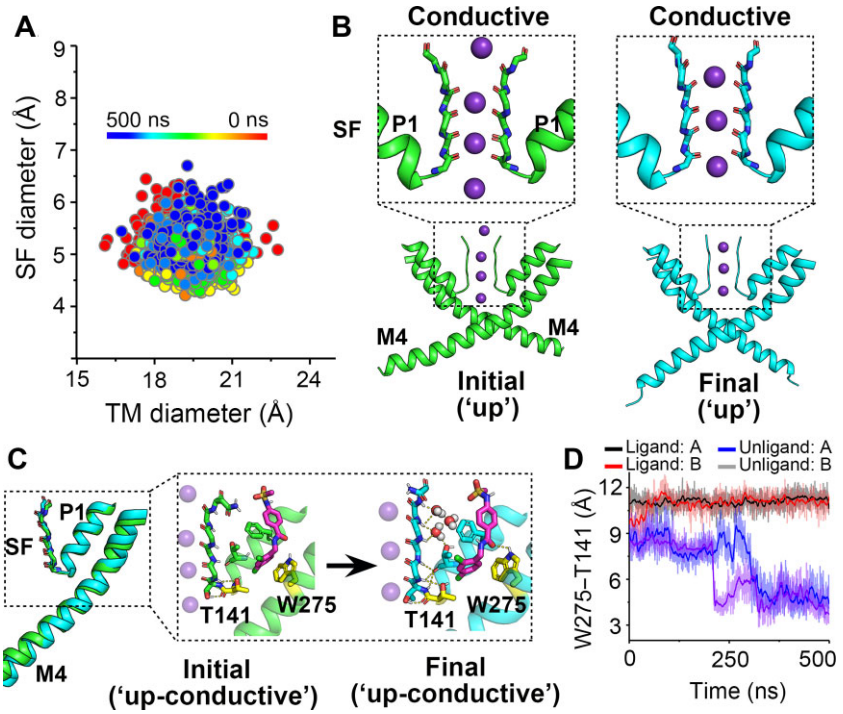

Figure 4 Conformation transitions of the TREK-1 channel in the SMD simulation of the ML335/TREK-1 complex. (**A**) Cluster analysis of the ML335/TREK-1 complex SMD trajectory with the distant SF diameter and TM diameter as two variables. (**B**) Typical conformations of the ML335/TREK-1 complex SMD trajectory. (**C**) The 'seesaw' movements of M4 and the influences of the movements on the networks within the filter region. (**D**) Time traces of distances between the indole NH group of W275 and the hydroxyl group of T141 during the ML335/TREK-1 system (liganded) or the TREK-1 system (unliganded) SMD simulation.

G137I is another gain-of-function mutation of the TREK-1 channel (Bagriantsev et al., 2012). The mechanism of this mutant associated with TREK-1 channel activation is also poorly understood. We performed a 500-ns SMD simulation on the G137I mutant and analyzed the movements of the M4 helix and the filter in the simulation (Figure 3F–J; Supplementary Figure S6). We observed that the transmembrane domain of the G137I channel only translated between the 'up' and 'down' structures but could not transfer to the 'deeper-down' structure (Figure 3G; Supplementary Figure S6A and B). Acting as a soft and small wedge between P1 and the M4 helix in the simulation, I137 partly limited the movements of the M4 N-terminus, one end of the 'seesaw' (Figure 3I). Consequently, I137 allosterically limited the movements of the M4 C-terminus, the other end of the 'seesaw'. Therefore, M4 could not transit to the 'deeper-down' conformation. In the filter region, W275 was too far from T141 to form interaction (Figure 3I and J). T141 still interacted with I143 and the networks stabilizing the conductive filter were retained.

These results explain why W275S and G137I act as gain-of-function mutations at the atomic level and indicate that 'C-type' gating could be modulated in various ways.

Action mechanisms of ML335 on channel gating

Small molecules may bind to pockets near the filter region (Lolicato et al., 2017; Liao et al., 2019; Schewe et al., 2019). The action mechanisms of these small molecules have not been well characterized. These small molecules may perturb the transitions of K2P channels from the open to closed state and thus increase the distribution probability of the open state. Here, we tried to study the action mechanisms of ML335, one of the small molecules that bind to a cryptic binding pocket near the filter of the TREK-1 channel (Lolicato et al., 2017). We built a simulation system of the ML335/TREK-1 complex in a POPC lipid bilayer and performed a 500-ns SMD simulation. We analyzed the movements of the M4 helix and the filter in the SMD simulation of the ML335/TREK-1 complex (Figure 4A and B; Supplementary Figure S7). The bound ML335 also acts as a wedge between P1 and the M4 helix (Figure 4C). However, this wedge is larger than the side chain of I137 in the mutant G137I. Compared with the gain-of-function mutation, ML335 limited the movements of the M4 N-terminus with a stronger effect. Meanwhile, this strong effect allosterically limited the movements of the M4 C-terminus, the other end of the 'seesaw'. As a result, although a force was applied on the M4 C-terminus, M4 remained in the 'up' conformation in the SMD simulation (Figure 4A and B; Supplementary Figure S7A and B). In the filter region, W275 was too far from T141 to form interaction (Figure 4C and D). Instead, the side chain of ML335 formed a stable hydrogen bond with the indole NH group of W275 (Figure 4C). The filter remained conductive in the SMD simulation on the ML335/TREK-1 complex (Figure 4B and C; Supplementary Figure S7C and D).

Together, in the presence of ML335, the 'seesaw' action of M4 was hindered and the transition of TREK-1 from the 'up' structure to other structures was restricted. ML402 is a derivative of ML335 that binds to a cryptic binding pocket (Lolicato et al., 2017). We found that ML402 regulates the TREK-1 channel by a mechanism similar to that of ML335 (Supplementary Figure S8).

Discussion

For the study of ion channels at the molecular level, solving protein structures and elucidating gating mechanisms are the two main researches. Along with the development of crystallography and cryo-EM methods, many structures of ion channels have been reported. However, to date, the understanding of channel gating is very preliminary. It is thought that using MD simulation to characterize the movements of ion channel gating is too challenging. Only the gating mechanism of a Kv channel has been well explored at the atomic level using MD simulations (Jensen et al., 2012). The current work clearly elucidated the 'C-type' gating mechanism of a K2P channel at the atomic level using MD simulations. Kv and K2P channels are quite different in their gating mechanisms. In the gating of Kv channels, movements of the S4 helix allosterically mediate the opening and closing of the gate at the helix-bundle crossing (Jensen et al., 2012). In the gating of K2P channels, movements of the M4 helix allosterically mediate the opening and closing of the filter gate.

Theoretically, as 'C-type' gating channels, K2P channels may have distinct dynamics in the filter conformation. Indeed, filter dynamics is the basis of K2P channel voltage sensing (Schewe et al., 2016), and small molecules may stimulate K2P function by reducing filter dynamics (Lolicato et al., 2017; Liao et al., 2019; Schewe et al., 2019). Therefore, a lot of effort has been made to find structural evidence for filter conformation changes. Harrigan et al. (2017) performed MD simulations on the TREK-2 channel and revealed a 'pinched' filter configuration using Markov modeling. The MD simulations of Brennecke and Groot suggested that the TREK-2 filter gates by a carbonyl flip (Brennecke and de Groot, 2018). Both MD studies indicated that the structure containing the less conductive filter is the 'down' structure. However, this conclusion driven by MD simulations is not consistent with crystal structures reported thus far. Crystallography studies show that the 'down' structure has a conductive filter similar to the 'up' structure. The current study solves this controversy. We find that the 'down' structure in MD simulations has a conductive filter, which is consistent with the results of crystallography studies. The structure with a nonconductive filter conformation belongs to another K2P structure, termed 'deeper-down', in which the M4 helix moves to a deeper down position. Without specific attention to M4 helix movements, it is difficult to discriminate the 'deeper-down' structure from the 'down' structure. Our study changes the K2P gating profile from 'up to down' to 'up to down to deeper-down'. The 'up' and 'deeper-down' structures represent the open and closed states of K2P channels. The 'down' structure is an intermediate state in gating processes.

The cross talk between transmembrane helices and the filter is crucial to linking stimuli and 'C-type' gating. In this study, we establish detailed mechanisms of the dynamic coupling between M4 and the filter. When the filter is conductive, T141 in P1 and I143 in SF1 form a stable hydrogen bond. Taking L282 as the fulcrum, the two termini of M4 couple to each other as a seesaw. Thus, the movements of the C-terminus to the 'deeper-down' position allosterically modulate the movements of the N-terminus. Then, the networks around the N-terminus changed. In particular, W275 in M4 participated in a hydrogen-bond network by forming an interaction with T141, whereas T141 lost its interaction with I143. Finally, the rearrangement of the hydrogen-bond networks induced filter conformation changes.

Ion channels are one of the three largest groups of drug targets. However, very few breakthroughs have been obtained in elucidating the action mechanisms of their modulators. First, it is difficult to resolve the complex structures of ion channels and their modulators. For potassium channels, the binding of small molecules in channels has only been observed in the structures of few members, such as KCNQ2 and TREK-1 (Lolicato et al., 2017; Li et al., 2021). Second, it is more difficult to characterize the effects of modulators on ion channel dynamics. Previously, researchers usually proposed that modulators may affect the dynamics of ion channel gates. This study revealed that ML335 influences the transition of TREK-1 from open to closed states, suggesting that compounds could activate ion channels by perturbing state transitions rather than by affecting the dynamics of gate.

Moreover, the findings of this work suggested that the 'C-type' gating could be allosterically modulated in many ways. The gain-of-function mutation W275S did not influence the movements of M4 helix. Instead, this mutation abolished the interaction between the movements of the M4 N-terminus and filter networks by removing the W275–T141 interaction. G137I is also a gain-of-function mutation that is located in the filter region. However, G137I showed action mechanisms different from those of W275S. This mutation influenced the movements of M4. M4 could not fluctuate between the 'up' and 'down' structures. As a small wedge between P1 and the M4 helix, I137 partly limited the movements of the M4 N-terminus, one end of the 'seesaw'. As a result, the M4 C-terminus, the other end of the 'seesaw', could not freely move to the 'deeper-down' conformation. Finally, we found that the action mechanisms of the activator ML335 are partially similar to those of the gain-of-function mutation G137I. This compound also acted as a wedge between P1 and the M4 helix. The difference is that ML335 is a larger wedge and has a stronger effect. In the ML335/TREK-1 complex, the M4 N-terminus could not move freely, and consequently, the C-terminus was restricted to the 'up' conformation. Overall, this study characterizes whether and how M4 helix movements modulate filter gating, the fundamental question of K2P channel 'C-type' gating. And this study revealed that mutations and ligands could regulate K2P gating by influencing the coupling between M4 and the filter. Dynamic 'C-type' gating can provide various action targets for channel modulator discovery.

Materials and methods

The simulation systems

An 'up' structure of the TREK-1 channel (PDB code: 6CQ8) (Lolicato et al., 2017) was used to construct the 'up' state related systems, including three unliganded systems (WT TREK-1 and mutants W275S and G137I) and two liganded systems (ML335/TREK-1 or ML402/TREK-1 complexes). The missing loops of the 'up' structure were built with RosettaRemodel (Huang et al., 2011), and the N- and C-termini were capped with methylamide and acetyl groups, respectively.

For the MD simulation of 'down' TREK-1, the initial 'down' structural model of TREK-1 was built using the homology-modeling method based on a 'down' structure of TREK-2 (PDB code: 4XDJ) (Dong et al., 2015). TREK-1 has a high sequence identity with TREK-2 (71%) (Supplementary Figure S3A). Multiple sequence alignments were generated by using the CLUSTALW web server (www.ebi.ac.uk/Tools/msa/clustalw2). Highly conserved residues were used to guide the alignment. The model was built by SWISS-MODEL based on the templates described above (Supplementary Figure S3B). We used Procheck (Laskowski et al., 1993) to evaluate the quality of the TREK-1 structural model, which showed that 98% of the residues were located in the rational region (Supplementary Figure S3C).

For each system, the channel was embedded in a POPC bilayer and then solved in a water box of $110 \times 110 \times 135$ Å^3. The PPM server was used to reorient the TREK-1 structure to ensure that the transmembrane domain of TREK-1 was well located in a lipid bilayer (Lomize et al., 2012). CHARMM-GUI was used to generate the configuration and topology of the simulation systems as well as the parameter files with the CHARMM36m force field (Wu et al., 2014; Lee et al., 2016). For the ML335/TREK-1 and ML402/TREK-1 systems, parameters of ML335 or ML402 were generated using the ParamChem web server and the CGenFF parameter set (Vanommeslaeghe et al., 2010). All systems were solved with ~34000 three-point (TIP3P) water molecules, and KCl corresponded to a concentration of 150 mM in the setup, totaling 150468–151236 atoms. Potassium ions were swapped into the channel selectivity filter (S0–S4 positions).

Conventional MD simulations

Conventional MD simulation was performed using the GROMACS5.1.2 and GROMACS2020 software packages (Hess et al., 2008). The channel structure was protonated according to the standard protonation states at pH 7. Isothermal and isobaric (NPT) ensemble and periodic boundary conditions were used in the simulations. To relieve unfavorable contacts, energy minimization was achieved using the steepest descent algorithm. Subsequently, we performed a 50-ns NPT equilibration simulation for each system to equilibrate the POPC lipid bilayer and the solvent with restraints (isotropic force constant $\kappa = 1 \times 10^3$ kJ/mol/nm^2) on the main chain of the TREK-1 channel. Finally, for each simulation, three independent 500-ns production runs were performed. In these simulations, the temperature parameters were coupled with the V-Resale method and maintained at 300 K (Bussi et al., 2007). The pressure was maintained at 1 bar using the Parrinello–Rahman method (Parrinello and Rahman, 1981) with $\tau_p = 1.0$ ps and a compressibility of 4.5×10^{-5}/bar. The SETTLE algorithm (Miyamoto and Kollman, 1992) and LINCS algorithm (Hess, 2008) were applied to the hydrogen-involved covalent bonds in water molecules and in other molecules, respectively. The time step was 2 fs. The initial velocity of particle motion was derived from the Maxwell distribution at 300 K. Electrostatic interactions were calculated using the particle-mesh Ewald (PME) algorithm with a real-space cutoff of 1.2 nm (Darden et al., 1993).

SMD simulations

For each system, SMD simulations were utilized to pull the Cα atoms of C-termini M4 helix (residues: 296–306) to simulate M4 helix movements. The Cap domains of the two chains of TREK-1 were treated as the reference group, and the C-terminal domains of the two chains of TREK-1 were treated as the pulling group. A tensile force parallel to the POPC phospholipid bimolecular layer was applied to the C-termini M4 helix of the TREK-1 channel. We tested a series of harmonic force constants as well as pulling speeds, and a harmonic force constant of 50 kJ/mol/nm^2 and a pulling speed of 0.1 Å/ns were found to be reasonable for the gating simulations, where conformation switching of the transmembrane domain was observed and the global protein structure was not disrupted in the 500-ns SMD simulation. The frames from MD/SMD trajectories were saved every 100 ps. Analysis of the trajectories was performed using GROMACS analysis tools. PyMOL (the PyMOL Molecular Graphics System, version 1.8, Schrödinger, LLC) was used to visualize the structure models and generate figures.

Supplementary material

Supplementary material is available at *Journal of Molecular Cell Biology* online.

Acknowledgements

We are thankful for the support of the ECNU Multifunctional Platform for Innovation (001).

Funding

This work was supported in part by the Ministry of Science and Technology (2018YFA0508100 to Q.Z. and J.G.), the National Natural Science Foundation of China (31800699 to Q.Z.), the Fundamental Research Funds for the Central Universities, and the 'XingFuZhiHua' funding of ECNU (44300-19311-542500/006 to H.Y.).

Conflict of interest: none declared.

Author contributions: H.Y. and Q.Z. conceived and designed this project. Q.Z., J.F., S.Z., P.G., S.L., and J.S. performed research. Q.Z., J.F., S.Z., P.G., and H.Y. analyzed data. Q.Z., J.G., and H.Y. provided critical feedback on the results and manuscript. Q.Z., J.F., and H.Y. wrote the paper.

References

Aryal, P., Jarerattanachat, V., Clausen, M.V., et al. (2017). Bilayer-mediated structural transitions control mechanosensitivity of the TREK-2 K2P channel. Structure *25*, 708–718.

Bagriantsev, S.N., Clark, K.A., and Minor, D.L. (2012). Metabolic and thermal stimuli control K_{2P}2.1 (TREK-1) through modular sensory and gating domains. EMBO J. *31*, 3297–3308.

Bagriantsev, S.N., Peyronnet, R., Clark, K.A., et al. (2011). Multiple modalities converge on a common gate to control K2P channel function. EMBO J. *30*, 3594–3606.

Brennecke, J.T., and de Groot, B.L. (2018). Mechanism of mechanosensitive gating of the TREK-2 potassium channel. Biophys. J. *114*, 1336–1343.

Brohawn, S.G., Campbell, E.B., and MacKinnon, R. (2013). Domain-swapped chain connectivity and gated membrane access in a Fab-mediated crystal of the human TRAAK K^+ channel. Proc. Natl Acad. Sci. USA *110*, 2129–2134.

Brohawn, S.G., Campbell, E.B., and MacKinnon, R. (2014). Physical mechanism for gating and mechanosensitivity of the human TRAAK K^+ channel. Nature *516*, 126–130.

Brohawn, S.G., del Marmol, J., and MacKinnon, R. (2012). Crystal structure of the human K2P TRAAK, a lipid- and mechano-sensitive K^+ ion channel. Science *335*, 436–441.

Bussi, G., Donadio, D., and Parrinello, M. (2007). Canonical sampling through velocity rescaling. J. Chem. Phys. *126*, 014101.

Cordero-Morales, J.F., Cuello, L.G., Zhao, Y.X., et al. (2006). Molecular determinants of gating at the potassium-channel selectivity filter. Nat. Struct. Mol. Biol. *13*, 311–318.

Cuello, L.G., Jogini, V., Cortes, D.M., et al. (2010a). Structural basis for the coupling between activation and inactivation gates in K^+ channels. Nature *466*, 272–275.

Cuello, L.G., Jogini, V., Cortes, D.M., et al. (2010b). Structural mechanism of C-type inactivation in K^+ channels. Nature *466*, 203–208.

Darden, T., York, D., and Pedersen, L. (1993). Particle mesh Ewald: an N·log(N) method for Ewald sums in large systems. J. Chem. Phys. *98*, 10089–10092.

Dong, Y.Y., Pike, A.C.W., Mackenzie, A., et al. (2015). K2P channel gating mechanisms revealed by structures of TREK-2 and a complex with Prozac. Science *347*, 1256–1259.

Douguet, D., and Honore, E. (2019). Mammalian mechanoelectrical transduction: structure and function of force-gated ion channels. Cell *179*, 340–354.

Feliciangeli, S., Chatelain, F.C., Bichet, D., et al. (2015). The family of K2P channels: salient structural and functional properties. J. Physiol. *593*, 2587–2603.

Goldstein, S.A.N., Bayliss, D.A., Kim, D., et al. (2005). International Union of Pharmacology. LV. Nomenclature and molecular relationships of two-P potassium channels. Pharmacol. Rev. *57*, 527–540.

Goldstein, S.A.N., Bockenhauer, D., O'Kelly, I., et al. (2001). Potassium leak channels and the KCNK family of two-P-domain subunits. Nat. Rev. Neurosci. *2*, 175–184.

Gonzalez, C., Baez-Nieto, D., Valencia, I., et al. (2012). K^+ channels: function-structural overview. Compr. Physiol. *2*, 2087–2149.

Harrigan, M.P., McKiernan, K.A., Shanmugasundaram, V., et al. (2017). Markov modeling reveals novel intracellular modulation of the human TREK-2 selectivity filter. Sci. Rep. *7*, 632.

Hess, B. (2008). P-LINCS: a parallel linear constraint solver for molecular simulation. J. Chem. Theory Comput. *4*, 116–122.

Hess, B., Kutzner, C., van der Spoel, D., et al. (2008). GROMACS 4: algorithms for highly efficient, load-balanced, and scalable molecular simulation. J. Chem. Theory Comput. *4*, 435–447.

Huang, P.S., Ban, Y.E.A., Richter, F., et al. (2011). RosettaRemodel: a generalized framework for flexible backbone protein design. PLoS One *6*, e24109.

Jensen, M.O., Jogini, V., Borhani, D.W., et al. (2012). Mechanism of voltage gating in potassium channels. Science *336*, 229–233.

Laskowski, R.A., MacArthur, M.W., Moss, D.S., et al. (1993). PROCHECK: a program to check the stereochemical quality of protein structures. J. Appl. Crystallogr. *26*, 283–291.

Lee, J., Cheng, X., Swails, J.M., et al. (2016). CHARMM-GUI input generator for NAMD, GROMACS, AMBER, OpenMM, and CHARMM/OpenMM simulations using the CHARMM36 additive force field. J. Chem. Theory Comput. *12*, 405–413.

Li, B.B., Rietmeijer, R.A., and Brohawn, S.G. (2020). Structural basis for pH gating of the two-pore domain K^+ channel TASK2. Nature *586*, 457–462.

Li, X.X., Zhang, Q.S., Guo, P.P., et al. (2021). Molecular basis for ligand activation of the human KCNQ2 channel. Cell Res. *31*, 52–61.

Liao, P., Qiu, Y., Mo, Y., et al. (2019). Selective activation of TWIK-related acid-sensitive K^+ 3 subunit-containing channels is analgesic in rodent models. Sci. Transl. Med. *11*, eaaw8434.

Lolicato, M., Arrigoni, C., Mori, T., et al. (2017). K2P2.1 (TREK-1)-activator complexes reveal a cryptic selectivity filter binding site. Nature *547*, 364–368.

Lolicato, M., Natale, A.M., Abderemane-Ali, F., et al. (2020). K2P channel C-type gating involves asymmetric selectivity filter order-disorder transitions. Sci. Adv. *6*, eabc9174.

Lolicato, M., Riegelhaupt, P.M., Arrigoni, C., et al. (2014). Transmembrane helix straightening and buckling underlies activation of mechanosensitive and thermosensitive K_{2P} channels. Neuron *84*, 1198–1212.

Lomize, M.A., Pogozheva, I.D., Joo, H., et al. (2012). OPM database and PPM web server: resources for positioning of proteins in membranes. Nucleic Acids Res. *40*, D370–D376.

Mathie, A., Al-Moubarak, E., and Veale, E.L. (2010). Gating of two pore domain potassium channels. J. Physiol. *588*, 3149–3156.

Mathie, A., Veale, E.L., Cunningham, K.P., et al. (2021). Two-pore domain potassium channels as drug targets: anesthesia and beyond. Annu. Rev. Pharmacol. Toxicol. *61*, 401–420.

Miyamoto, S., and Kollman, P.A. (1992). Settle: an analytical version of the SHAKE and RATTLE algorithm for rigid water models. J. Comput. Chem. *13*, 952–962.

Parrinello, M., and Rahman, A. (1981). Polymorphic transitions in single crystals: a new molecular dynamics method. J. Appl. Phys. *52*, 7182–7190.

Piechotta, P.L., Rapedius, M., Stansfeld, P.J., et al. (2011). The pore structure and gating mechanism of K2P channels. EMBO J. *30*, 3607–3619.

Pope, L., Lolicato, M., and Minor, D.L., Jr. (2020). Polynuclear ruthenium amines inhibit K2P channels via a 'finger in the dam' mechanism. Cell Chem. Biol. *27*, 511–524.e4.

Rodstrom, K.E.J., Kiper, A.K., Zhang, W., et al. (2020). A lower X-gate in TASK channels traps inhibitors within the vestibule. Nature *582*, 443–447.

Schewe, M., Nematian-Ardestani, E., Sun, H., et al. (2016). A non-canonical voltage-sensing mechanism controls gating in K2P K^+ channels. Cell *164*, 937–949.

Schewe, M., Sun, H., Mert, U., et al. (2019). A pharmacological master key mechanism that unlocks the selectivity filter gate in K^+ channels. Science *363*, 875–880.

Tian, C., Zhu, R., Zhu, L., et al. (2014). Potassium channels: structures, diseases, and modulators. Chem. Biol. Drug Des. *83*, 1–26.

Vanommeslaeghe, K., Hatcher, E., Acharya, C., et al. (2010). CHARMM general force field: a force field for drug-like molecules compatible with the CHARMM all-atom additive biological force fields. J. Comput. Chem. *31*, 671–690.

Wu, E.L., Cheng, X., Jo, S., et al. (2014). CHARMM-GUI membrane builder toward realistic biological membrane simulations. J. Comput. Chem. *35*, 1997–2004.

Wulff, H., Castle, N.A., and Pardo, L.A. (2009). Voltage-gated potassium channels as therapeutic targets. Nat. Rev. Drug Discov. *8*, 982–1001.